

UCLA

UCLA Previously Published Works

Title

Involvement of zebrafish Na⁺,K⁺ ATPase in myocardial cell junction maintenance

Permalink

<https://escholarship.org/uc/item/8f21d3zg>

Journal

Journal of Cell Biology, 176(2)

ISSN

0021-9525

Authors

Cibrián-Uhalte, Elena
Langenbacher, Adam
Shu, Xiaodong
[et al.](#)

Publication Date

2007-01-15

DOI

10.1083/jcb.200606116

Peer reviewed

Involvement of zebrafish Na⁺,K⁺ ATPase in myocardial cell junction maintenance

Elena Cibrián-Uhalte,¹ Adam Langenbacher,² Xiaodong Shu,² Jau-Nian Chen,^{2,3,4} and Salim Abdelilah-Seyfried¹

¹Max Delbrück Center for Molecular Medicine, 13125 Berlin, Germany

²Department of Molecular, Cell, and Developmental Biology, ³Jonsson Comprehensive Cancer Center, and ⁴Molecular Biology Institute, University of California, Los Angeles, Los Angeles, CA 90095

Na⁺,K⁺ ATPase is an essential ion pump involved in regulating ionic concentrations within epithelial cells. The zebrafish *heart and mind* (*had*) mutation, which disrupts the α 1B1 subunit of Na⁺,K⁺ ATPase, causes heart tube elongation defects and other developmental abnormalities that are reminiscent of several epithelial cell polarity mutants, including *nagie oko* (*nok*). We demonstrate genetic interactions between *had* and *nok* in maintaining Zonula occludens-1 (ZO-1)-positive

junction belts within myocardial cells. Functional tests and pharmacological inhibition experiments demonstrate that Na⁺,K⁺ ATPase activity is positively regulated via an N-terminal phosphorylation site that is necessary for correct heart morphogenesis to occur, and that maintenance of ZO-1 junction belts requires ion pump activity. These findings suggest that the correct ionic balance of myocardial cells is essential for the maintenance of epithelial integrity during heart morphogenesis.

Introduction

The Na⁺,K⁺ ATPase, or Na pump, is primarily involved in the generation of Na⁺ and K⁺ gradients across plasma membranes and in the determination of cytoplasmic Na⁺ levels. Its function is tightly coupled to the regulation of cell volume and intracellular pH and Ca²⁺ levels through the activities of the Na⁺/H⁺ and Na⁺/Ca²⁺ exchangers (for reviews see Blanco and Mercer, 1998; Therien and Blostein, 2000). In addition to maintaining the osmotic balance of the cell, Na⁺,K⁺ ATPase functions as a scaffold for proteins involved in different functions, ranging from signal transduction to the cytoskeleton (Lopina, 2000).

Studies in invertebrate models and tissue culture systems have suggested an involvement of Na⁺,K⁺ ATPase in junctional complex formation. In *Drosophila melanogaster*, the Na⁺,K⁺ ATPase α and β subunits are essential for barrier function of the septate junction, which is a structure that functions as a paracellular diffusion barrier similar to the vertebrate tight junction (Genova and Fehon, 2003; Paul et al., 2003). Colocalization and functional studies demonstrated that Na⁺,K⁺ ATPase is essential for correct localization of several other septate junction proteins without affecting epithelial cell polarity.

In vertebrates, a Ca²⁺-switch assay in MDCK cells suggested that Na⁺,K⁺ ATPase activity may be essential for tight junction formation and development of polarity (Rajasekaran et al., 2001a). Blockage of the pump function using ouabain and by K⁺ depletion (which abolishes the steep K⁺ gradient required for pump function) caused the specific and reversible inhibition of tight junction formation, whereas adherens junctions were not affected. Similarly, the inhibition of Na⁺,K⁺ ATPase affected the tight junction structure and transmembrane permeability of human retinal pigment epithelial cells (Rajasekaran et al., 2003).

The zebrafish α 1B1 subunit of Na⁺,K⁺ ATPase is encoded by the *heart and mind* (*had*) locus and is required for heart morphogenesis and brain ventricle formation during embryonic development of the zebrafish (Shu et al., 2003; Yuan and Joseph, 2004; Lowery and Sive, 2005). The *had* mutant heart phenotype is characterized by a delay in heart cone formation and transformation of this cone into the elongated heart tube, a phenotype reminiscent of the *heart and soul* (*has*)/atypical protein kinase *ci* (*apkc*c*i*) and *nagie oko* (*nok*)/MAGUK p55 subfamily member 5 (*mpp5*) mutant and morphant phenotypes (Yelon et al., 1999; Horne-Badovinac et al., 2001; Peterson et al., 2001; Rohr et al., 2006). Has/aPKC ϵ is required for the establishment of apical-basal polarity of epithelial cells and is an essential component of a tight junction-associated protein complex that includes the PDZ domain, containing scaffolding proteins Par3 and Par6. Nok/Mpp5 is a tight junction-associated scaffolding protein of the apical Crumbs polarity complex (Rohr et al., 2006).

Correspondence to Salim Abdelilah-Seyfried: salim@mdc-berlin.de; or Jau-Nian Chen: chenjn@mcdb.ucla.edu

Abbreviations used in this paper: cmlc2, cardiac myosin light chain 2; hpf, hours postfertilization; Had, heart and mind; Has, heart and soul; MO, morpholino antisense oligonucleotide; Nok, Nagie oko; wt, wild type; ZO-1, Zonula occludens-1.

The online version of this article contains supplemental material.

Physical interactions between the Crumbs–Nok/Mpp5 and the Par3–aPKC–Par6 protein complexes have been previously described (Hurd et al., 2003; Nam and Choi, 2003; Wang et al., 2004). Consistent with a function in apical–basal cell polarity, loss of *haslapkc1* and *nok/mpp5* using morpholino antisense oligonucleotides (MO) causes a disruption of Zonula occludens-1 (ZO-1)–positive apical junctions within the embryonic myocardium (Rohr et al., 2006).

The role of Na⁺,K⁺ ATPase during the development of vertebrate epithelia is poorly understood. We investigate function and regulatory mechanisms of this important ion pump during zebrafish heart morphogenesis. Our analysis demonstrates genetic interactions between *had/Na⁺,K⁺ ATPase* and *nok* in the maintenance of ZO-1–positive junction belts within myocardial cells. Functional analysis of regulatory and catalytic ATPase mutants, as well as pharmacological inhibition experiments, demonstrate the importance of correct ionic balance controlled by the Na pump for the maintenance of myocardial integrity.

Results

Had/Na⁺,K⁺ ATPase and Nok/Mpp5 interact in the maintenance of apical myocardial junctions

Zygotic *nok^{m520}* and *had^{al}* mutants display similar heart tube elongation defects, which led us to evaluate the possibility

that both genes interact in the maintenance of apical junctions within myocardial cells. To visualize the effects of *nok/mpp5* and *had* on myocardial development, we introduced a transgene that expresses GFP under the control of the *cardiac myosin light chain 2 (cmlc2)* promoter region (*Tg[cmlc2:GFP]*; Huang et al., 2003) into the *nok^{m520}* mutant background and injected clutches of these fish with *had*MO (*nok* mutants were recognized by their prominent retinal pigment epithelial phenotype). An antibody against the junctional protein ZO-1 was used to assess the integrity of apical myocardial junctions. In comparison to wild type (wt), both *nok^{m520}* mutants and *had* morphants displayed strongly shortened heart tubes by 36 h postfertilization (hpf; Fig. 1, A–C), but displayed intact apical ZO-1 junction belts (Fig. 1, B' and C'; *nok^{m520}*, *n* = 12/12 hearts with intact ZO-1 junction belts; *had* morphants, *n* = 10/10 hearts with intact ZO-1 junction belts). Loss of both genes (*nok^{m520};had* double mutant/morphants) resulted in a severe cardiac elongation defect that was stronger than the individual loss of function phenotypes (Fig. 1 D). In some cases, the heart was small and positioned at the midline, suggesting that morphogenesis was arrested at the heart cone stage, a phenotype reminiscent of *haslapkc1* mutants. This phenotype correlated with severely disrupted apical ZO-1 junction belts (Fig. 1 D'; *n* = 0/8 hearts with intact ZO-1 junction belts). In comparison, 16-somite stage embryos of different genetic backgrounds (including *nok^{m520};had* double mutant/morphants) exhibited intact apical

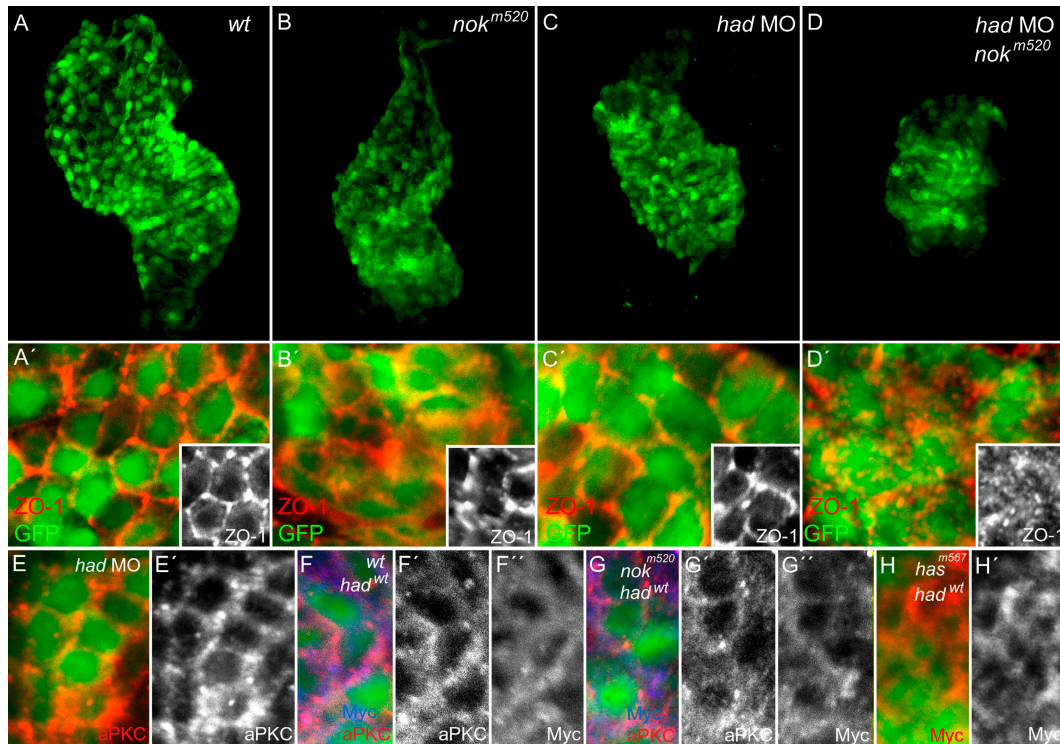


Figure 1. Genetic interactions of *had* and *nok* during heart morphogenesis. Reconstructions of confocal z-stack sections of embryonic hearts. (A–D) Morphology of transgenic *Tg[cmlc2:GFP]* embryonic hearts in different genetic backgrounds at 34–36 hpf. (A'–D') Localization of ZO-1 in myocardial cells at 36 hpf in different genetic backgrounds and details thereof (insets). Whereas ZO-1–positive junction belts are present in *nok^{m520}* mutants (B and B') and *had* morphants (C and C'), they are severely disrupted upon loss of both genes (D and D'). (E and E') aPKCs are correctly localized to the membrane in *had* MO hearts at 34–36 hpf. (F–H) Embryos of different genetic backgrounds injected with mRNA encoding Myc-tagged Had/Na⁺,K⁺ ATPase were used to detect the subcellular localization of the fusion protein, which remains at the membrane in wt (F), *nok^{m520}* (G), and *has^{m567}* mutants (H).

ZO-1-positive junction belts (Fig. S1, available at <http://www.jcb.org/cgi/content/full/jcb.200606116/DC1>).

We next investigated whether interaction between Had/Na⁺,K⁺ ATPase and Nok/Mpp5 is via regulation of each other's subcellular localization. To test this possibility, we analyzed *had* morphants using an antibody against aPKC ζ and ζ as a marker for the apical Nok/Mpp5-Par6-aPKC protein complex (Suzuki and Ohno, 2006; Rohr et al., 2006) and detected normal localization at the membrane at 34–36 hpf (Fig. 1 E). For the converse analysis, we characterized the subcellular localization of Myc-tagged Had/Na⁺,K⁺ ATPase in wt (Fig. 1 F), *nok*^{m520} mutant (Fig. 1 G), and *has*^{m567} mutant backgrounds (Fig. 1 H). In both mutants, the fusion protein was correctly localized to the membrane. Therefore, Had/Na⁺,K⁺ ATPase and Nok/Mpp5 do not affect each other's membrane association. However, the squamous morphology of cardiomyocytes prevented an unambiguous characterization of protein distribution along the apical-basal axis.

At the 20-somite stage, myocardial cells exhibit cuboidal shapes and are highly polarized. As shown in Fig. 2, *had* morphants displayed correctly localized aPKC and ZO-1 junction belts (Fig. 2 B), suggesting that apical-basal polarity was not impaired. However, whereas aPKC was strongly localized to apical junction belts in wt cardiomyocytes (Fig. 2 C), it was clearly displaced in *nok* morphant cardiomyocytes, indicating a loss of apical-basal polarity (Fig. 2 E). In addition, we visualized the subcellular localization of Had/Na⁺,K⁺ ATPase by analyzing the distribution of the exogenous Myc-tagged Had/Na⁺,K⁺ ATPase. Although we consistently detected low levels of Myc-tagged Had/Na⁺,K⁺ ATPase localized to the membrane of wt cardiomyocytes (Fig. 2, C and C'), high levels of Myc-tagged Had/Na⁺,K⁺ ATPase were detected around the circumference of myocardial cells in both *has* and *nok* morphants (Fig. 2, D and E; five embryos analyzed for each genotype). These findings suggest that one way by which Nok/Mpp5 and Has/aPKC ζ affect Had/Na⁺,K⁺ ATPase could be by directing its subcellular localization.

An N-terminal phosphorylation site of Had/Na⁺,K⁺ ATPase is required for correct activity during heart tube elongation

The finding that Had/Na⁺,K⁺ ATPase and Nok/Mpp5 interact in the maintenance of apical myocardial junctions raised the intriguing possibility that the ionic balance produced by the Na pump is critical in this process. To functionally characterize the role of the ion pump function, we first investigated the mechanisms by which Had/Na⁺,K⁺ ATPase activity is regulated during heart morphogenesis. We initiated this characterization by a sequence comparison of the two functionally divergent α 1B1 (Had) and α 2 subunits of Na⁺,K⁺ ATPase, which share a high degree of similarity throughout the entire peptide (84% identity), except for the first cytoplasmic domain (67% identity among the first 98 residues). In contrast to *had* mutants, embryos deficient for the α 2 subunit display cardiac laterality rather than primitive heart tube formation defects (Shu et al., 2003). To test the relevance of N-terminal regulatory elements for α 1B1 subunit function, we generated two expression constructs that encode chimeric proteins between the α 1B1 and α 2 subunits. The first construct encodes a chimeric protein containing the 98 N-terminal residues of the α 1B1 subunit fused to the α 2 C-terminal rest (NIC2), whereas the second construct encodes the reciprocal chimeric protein containing the N-terminal domain of the α 2 subunit fused with the α 1B1 C-terminal rest (N2C1). Although 77% of *had*^{dal} mutants injected with the NIC2 mRNA developed a normal heart tube ($n = 35/45$ embryos; rescue efficiency is similar to wt *had* mRNA [81%, $n = 34/42$ embryos]; $P > 0.5$), *had*^{dal} mutants could not be rescued by injection of N2C1 mRNA ($n = 0/41$ embryos; 0% rescue efficiency). This structure function analysis points at regulatory elements important for α 1B1 subunit function within the N-terminal end of the protein.

Intriguingly, there are several conserved aPKC consensus phosphorylation sites within the 25 most N-terminal residues of the α 1B1 subunit that are missing within the α 2 subunit (Fig. 3, B and C). To assess whether heart tube elongation depends on

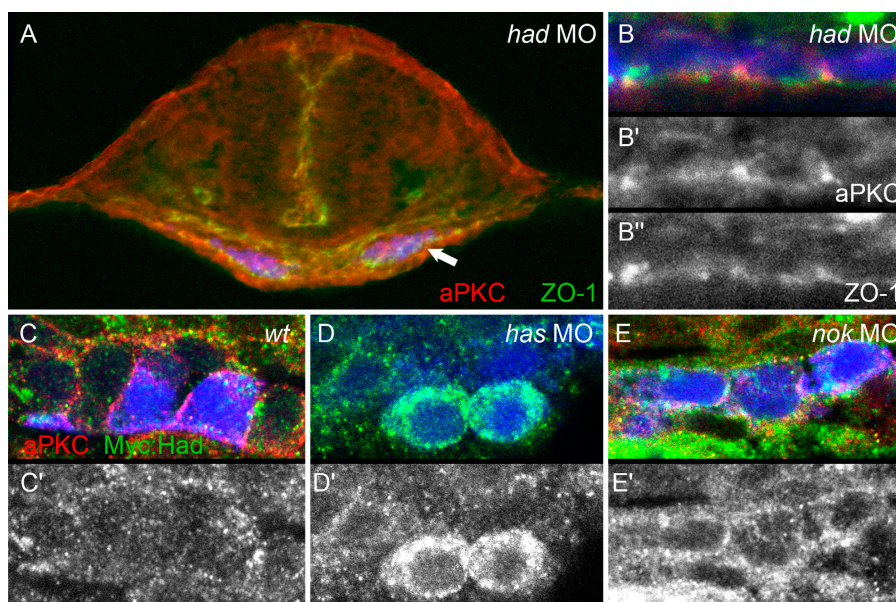


Figure 2. Effects of *had*, *has*, and *nok* morphants on myocardial apical-basal polarity at the 20-somite stage. Transverse sections of heart cone stage (20-somite) embryos. GFP is false-colored in blue; aPKC, red (A–C and E) or gray (B'); Myc::Had, green (C–E) or gray (C'–E'); ZO-1, green (A and B) or gray (B''). (A) *had* morphant with a section plane through the middle of the heart cone. The two bilateral wings of myocardial cells are blue. Arrow indicates the lateral portion of the myocardial field that was used for detail images within the various genetic backgrounds. (B, B', and B'') *had* morphants are correctly polarized and display apical ZO-1- and aPKC-positive spots. (C and C') In wt myocardial cells, levels of Myc::Had/Na⁺,K⁺ ATPase are low, and a clear localization pattern is not apparent. (D and D') *has* morphant myocardial cells exhibit higher levels of Myc::Had/Na⁺,K⁺ ATPase, which is localized around the circumference of cells. (E and E') Similarly, *nok* morphants display localization of Myc::Had/Na⁺,K⁺ ATPase and aPKC around the entire myocardial circumferences, which is indicative of loss of apical-basal polarity within these cells.

the regulation of Had/Na⁺,K⁺ ATPase via one or more of these three N-terminal aPKC consensus phosphorylation sites, we generated expression constructs with point mutations that encode for phosphorylation-deficient forms of the protein (exchanges of Ser residues for Ala: *had*^{S16A}, *had*^{S23A}, and *had*^{S25A}), as well as a triple-mutant nonphosphorylatable form (*had*^{3A}; Fig. 3 C). We assayed the effects of these mutations on heart tube elongation by their ability to rescue the *had*^{Δ1} mutant phenotype and found that injection of *had*^{S16A}, *had*^{S23A}, and a phosphomimetic mutant mRNA with an exchange of Ser25 to Glu (*had*^{S25E}) yielded a robust rescue of the heart tube elongation defects in most embryos that was comparable to *had*^{wt} mRNA (Fig. 3, F, I, and J), whereas *had*^{S25A} and *had*^{3A} mRNAs displayed significantly reduced rescue efficiencies (Fig. 3, G, H, and J). Thus, some of the biological activity of Had/Na⁺,K⁺ ATPase during heart tube elongation critically depends on Ser25.

The zebrafish mutation *has/lapkcι* prevents normal heart tube elongation (Yelon et al., 1999), and our data showed that Had/Na⁺,K⁺ ATPase is mislocalized in *has* morphants, raising the possibility that Had/Na⁺,K⁺ ATPase is a direct target of

Has/aPKCι. Therefore, we conducted a direct phosphorylation assay, but did not detect any phosphorylation among the first 98 amino acids of Had/Na⁺,K⁺ ATPase by either human recombinant aPKCζ or zebrafish Has/aPKCι (Fig. S2, available at <http://www.jcb.org/cgi/content/full/jcb.200606116/DC1>). This finding suggests that the N-terminal regulatory domain Had/Na⁺,K⁺ ATPase is not a direct target of Has/aPKCι.

Direct phosphorylation of rat Na⁺,K⁺ ATPase by aPKC at Ser23 of the α subunit is an important mechanism by which the pump activity is regulated (Vasilets et al., 1990, 1997, 1999; Bertorello et al., 1991; Chibalin et al., 1997, 1998). Phosphorylation at this residue causes the increased internalization of the Na pump into endocytic vesicles, effectively resulting in a reduced ion pump function at the plasma membrane. To assess whether reduced activity of Had^{3A} could be the consequence of a changed subcellular protein distribution compared with the wt form, we analyzed the membrane association of the mutant and wt Myc-tagged fusion proteins. Western blot analysis demonstrated that the nonphosphorylatable form of the protein was enriched within the membrane and cytoskeletal fraction of embryonic extracts similar to

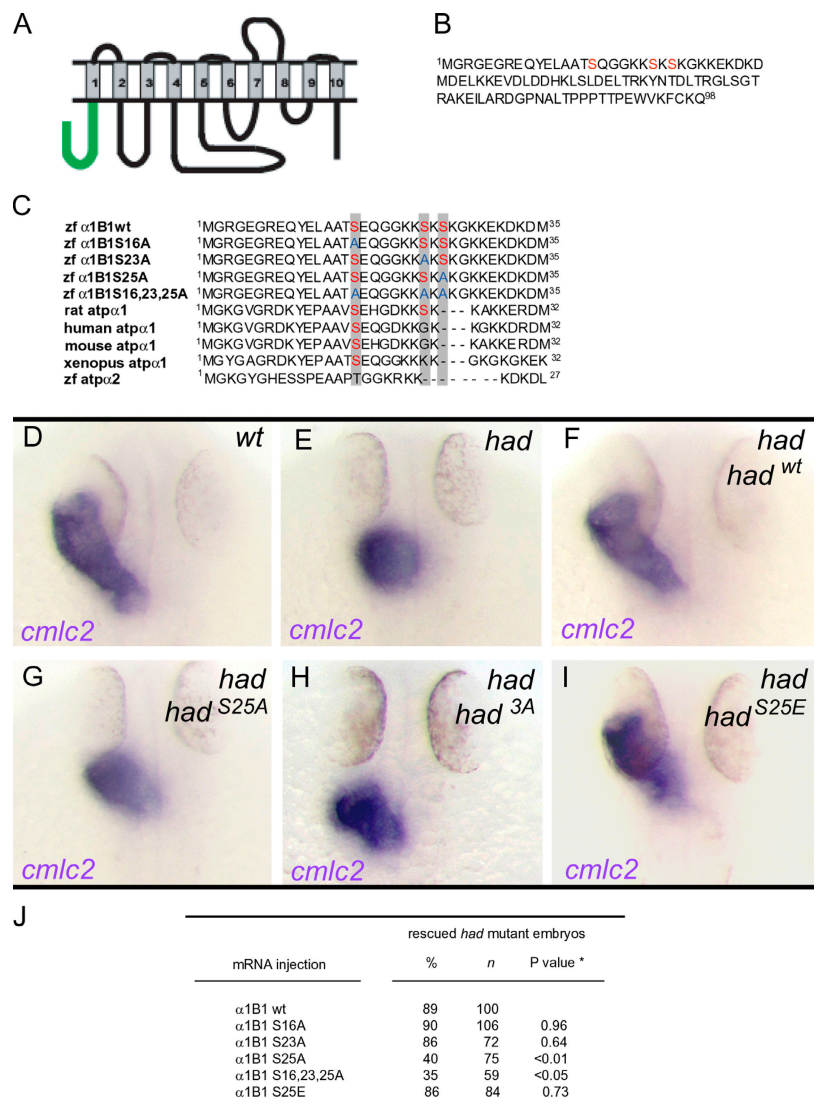


Figure 3. N-terminal Ser25 is required for correct activity of Had/Na⁺,K⁺ ATPase during heart tube elongation. (A) Predicted structure of the Na⁺,K⁺ ATPase α1B1 subunit. The N-terminal intracellular tail (98 residues) is shown in green. Transmembrane domains are numbered. (B) Protein sequence of the Had/Na⁺,K⁺ ATPase N-terminal intracellular tail (first 98 residues). Three predicted aPKC phosphorylation target sites are shown in red. (C) Sequence alignment of the first 35 residues of the N-terminal intracellular tail of zebrafish wt and mutated forms of Na⁺,K⁺ ATPase α1B1, rat Na⁺,K⁺ ATPase α1, human Na⁺,K⁺ ATPase α1, mouse Na⁺,K⁺ ATPase α1, *X. laevis* Na⁺,K⁺ ATPase α1, and zebrafish Na⁺,K⁺ ATPase α2. Predicted aPKC phosphorylation target sites Ser16, which is conserved among all species, Ser23, which is conserved among rat and zebrafish, and Ser25, which is only present in zebrafish, are shown in red. Serine residues mutated to alanine are shown in blue. (D–I) Dorsal view of embryos at 34–36 hpf analyzed for expression of myocardial marker *cmlc2*. Heart tube elongation defects in *had*^{Δ1} mutant embryos that were injected with wt or mutant forms of *had* mRNA. (J) Quantifications of the rescue of *had*^{Δ1} mutant heart tube defects after injection of wt or mutant forms of *had* mRNA. Statistical P values for rescue efficiency of different mutant mRNAs compared with wt mRNA rescue efficiency are shown. P values <0.05 are considered statistically significant.

* Compared to α1B1wt

the wt form (Fig. 4 A). To further quantify and compare the relative membrane distribution of wt and nonphosphorylatable forms of Had/Na⁺,K⁺ ATPase, we measured the relative amounts of protein from three independently prepared protein fractionations (one of which is shown in Fig. 4 A). Indeed, the relative membrane fractions accounted for 65.5 ± 5.3% SD for wt and 64.5 ± 6.7% SD for the nonphosphorylatable mutant forms of the protein, and demonstrated that the relative membrane association of Had/Na⁺,K⁺ ATPase is not affected by Ser25 phosphorylation. In immunohistochemical stainings, both wt and nonphosphorylatable forms of the protein were largely associated with the outer cell membrane of myocardial cells (Fig. 4, B and C). Quantification of the relative membrane distributions of protein based on these stainings accounted for 60.8 ± 4.4% SD for wt (*n* = 45 myocardial cells) and 61.9 ± 4.7% SD for the nonphosphorylatable mutant form (*n* = 50 myocardial cells). These observations suggest that, during zebrafish embryogenesis, regulation via Ser25 does not cause a substantial removal of the Na pump from the outer cell membrane; rather, they suggest that phosphorylation of Ser25 positively controls ion pump activity at the outer cell membrane.

Evidence for a role of the Had/Na⁺,K⁺ ATPase ion pump activity in the maintenance of myocardial cell junctions

To further explore the possibility that the ionic balance produced by the Na pump is critical in the maintenance of myocardial

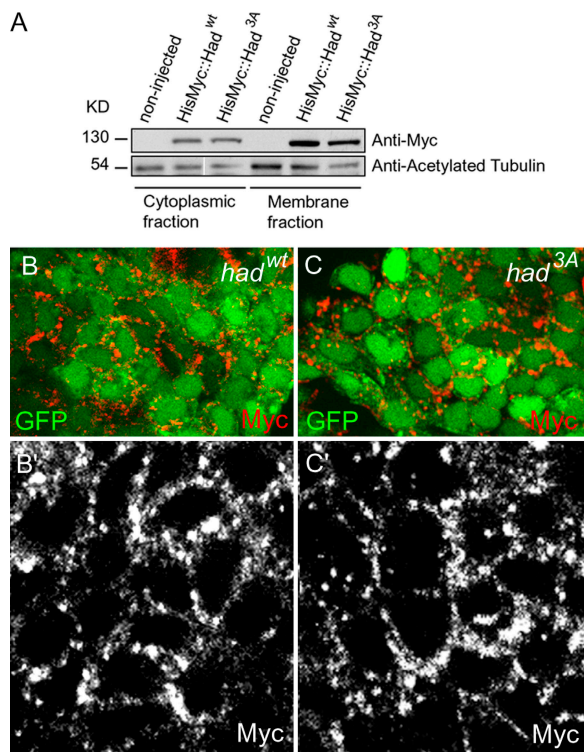


Figure 4. **The N-terminal phosphorylation state of Had/Na⁺,K⁺ ATPase does not affect membrane association.** (A) Western blot of 32 hpf embryonic extracts shows that HisMyc::Had^{wt} and HisMyc::Had^{3A} are enriched within the membrane and cytoskeletal fraction. (B and C) Confocal fluorescence microscopic images. Myocardial wt cells expressing HisMyc::Had^{wt} (B and B') and HisMyc::Had^{3A} (C and C'). Both recombinant forms of the Na pump are mostly localized at the outer cell membrane.

apical junction belts, we first produced a mutant form of Had/Na⁺,K⁺ ATPase that specifically affects the ATPase catalytic activity, which is required to pump Na across the plasma membrane and tested whether this activity is essential for regulating primitive heart tube formation. We replaced the aspartic acid at position 379 by an asparagine (Had^{D379N}) to produce a mutant protein that has previously been shown to abolish the binding of ATP to Na⁺,K⁺ ATPase in cultured cells (Ohtsubo et al., 1990). Injection of *had*^{D379N} mRNA into *had*^{la1} mutant embryos could not rescue the primitive heart tube phenotype (only 4% of injected mutants develop a heart tube, *n* = 40). Nevertheless, the protein was stable and could be detected on Western blots (Fig. S3, available at <http://www.jcb.org/cgi/content/full/jcb.200606116/DC1>). Therefore, ATPase catalytic activity is required for heart tube elongation.

Next, we analyzed ATPase catalytic and regulatory mutants in the genetic interaction with *nok*. Low levels of *had*MO (2.5 ng) were coinjected together with *HisMyc::had*^{wt}, *HisMyc::had*^{3A}, or *HisMyc::had*^{D379N} mRNA into *nok*^{m520} mutants, and antibodies against the junctional protein ZO-1 were used to assess the integrity of apical myocardial junctions at 32 hpf. Indeed, unlike the control *nok*^{m520};*had*^{wt} single-mutant embryos, *nok*^{m520};*had*^{3A} and *nok*^{m520};*had*^{D379N} double mutant/morphants displayed disrupted ZO-1 junctional belts (Fig. 5, A–C). Similarly, *nok*^{m520} embryos treated with ouabain, which is a potent inhibitor of Na⁺,K⁺ ATPase activity, resulted in a loss of ZO-1 junction belts (Fig. 5 D). Together, these findings suggest that

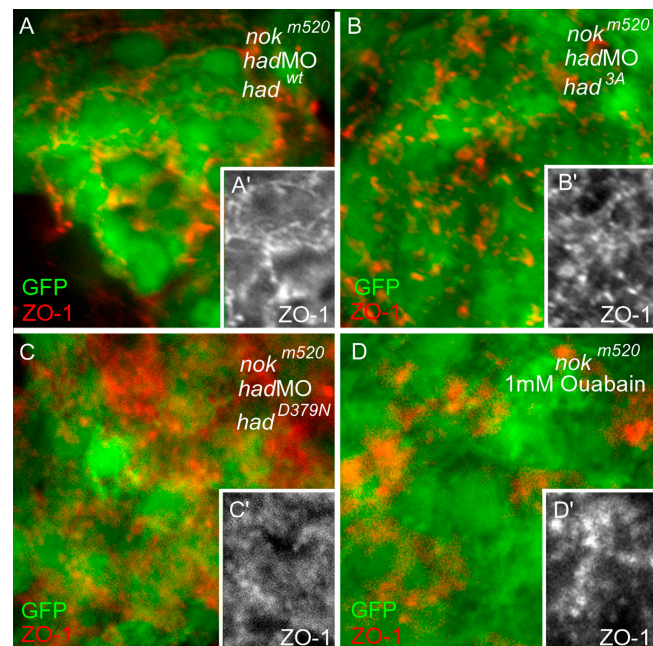


Figure 5. **Genetic interactions of a Had/Na⁺,K⁺ ATPase regulatory and catalytic mutants with Nok/Mpp5 in the maintenance of ZO-1-positive junction belts.** Reconstructions of confocal z-stack sections of embryonic hearts. (A–D) *nok*^{m520} mutants transgenic for *Tg(cmlc2:GFP)* were injected with *had*MO together with *HisMyc::had*^{wt} (A), *HisMyc::had*^{3A} (B), *HisMyc::had*^{D379N} mRNA (C), or treated with 1 mM ouabain (D). *HisMyc::had*^{wt} mRNA rescues the disruption of ZO-1-positive junction belts in *nok*^{m520} mutants (A'), unlike *HisMyc::had*^{3A} (B') and *HisMyc::had*^{D379N} mutant mRNA, which does not (C'), or ouabain treatment (D').

the interaction between Nok/Mpp5 and Had/Na⁺,K⁺ ATPase in the maintenance of myocardial ZO-1 junction belts requires the Na pump function, and that correct ionic balance contributes to the maintenance of myocardial integrity.

Discussion

Our study has demonstrated an essential role of the ion pump function of Had/Na⁺,K⁺ ATPase for the maintenance of apical ZO-1 junction belts. Independent mutations that affect Na⁺,K⁺ ATPase regulation and catalytic activity, which is required to pump Na across the plasma membrane, provide strong evidence for the importance of correct ionic balance of myocardial cells for cell polarity and heart morphogenesis. We have shown that impaired ion pump function enhances the loss of apical ZO-1-positive junction belts in a *nok* mutant background (Fig. 6). These findings are corroborated by previous studies in MDCK cells that suggested a critical requirement of the Na pump in the establishment of epithelial cell polarity and in the formation of tight junctions in a calcium switch assay (Rajasekaran et al., 2001a,b). These studies also provided evidence for synergistic activities between the adherens junction protein E-cadherin and Na⁺,K⁺ ATPase in the formation of continuous ZO-1-positive tight junction belts that are similar to our observation of genetic interactions between *had* and *nok* during zebrafish heart morphogenesis (Rajasekaran et al., 1996, 2001b).

There has been considerable interest in Na⁺,K⁺ ATPase from a physiological standpoint. However, little is known about the regulation or cell biological functions of the Na pump in the context of early vertebrate development. Our study reveals that Ser25 within the α1B1 subunit positively affects its function. Loss of rescue activity associated with a Ser25Ala mutation and normal rescue activity associated with a Ser25Glu phosphomimetic mutation suggest a positive regulatory mechanism for Na⁺,K⁺ ATPase function during zebrafish heart development.

Studies using D1-transfected OK cells (a cell line derived from Opossum kidney) and *Xenopus laevis* oocytes suggest that an important mechanism of regulation of Na pump function is via aPKC-mediated inhibition involving phosphorylation of Ser23 of rat. This phosphorylation event results in the internalization of the Na pump via increased endocytosis and, therefore, effective inactivation (Chibalin et al., 1997, 1998; Vasilets et al., 1990, 1997, 1999). According to Hug and Sarre (1993), there are multiple potential phosphorylation motifs present within the zebrafish Na⁺,K⁺ ATPase α1B1 subunit that may be phosphorylated by various isoforms of aPKC. Alternative potential phosphorylation events could be the basis for variable effects of aPKC on ion pump activity reported in the literature, and also for the seemingly different results obtained in our study (Therien and Blostein, 2000). We find that during early zebrafish development, the phosphorylation state of the N-terminal regulatory residues of Had/Na⁺,K⁺ ATPase does not affect the relative membrane association. The experimental model system established in this study provides a framework for detailed approaches to dissect the molecular components involved in the regulation of the Na pump during heart morphogenesis and development in general.

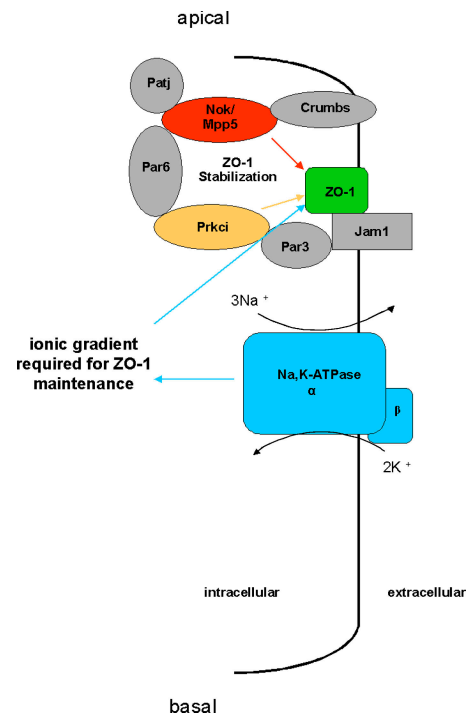


Figure 6. Model for the interactions between Nok/Mpp5 and Had/Na⁺,K⁺ ATPase in the maintenance of apical junction belts within myocardial cells. The ion pump activity of Had/Na⁺,K⁺ ATPase, which maintains the ionic balance of myocardial cells, interacts with the tight junction-associated protein Nok/Mpp5, a scaffolding partner of apical Crumbs and Par6-aPKC_ϵ protein complexes, in the stabilization of apical ZO-1-positive junctional belts.

In this study, we found that the apical-basal polarity is lost in myocardial cells of *has* morphants at the 20-somite stage, and that Had/Na⁺,K⁺ ATPase is mislocalized along the entire outer cell membrane. These findings are consistent with a previous study showing that the polarized distribution of Na⁺,K⁺ ATPase in MDCK cells is disrupted upon treatment with a dominant-negative form of aPKC (Suzuki et al., 2001) and support the notion that proper subcellular distribution of Had/Na⁺,K⁺ ATPase is dependent on the activity of Has/aPKC_ϵ. Because our data demonstrate that the phosphorylation of Ser25 is critical for heart tube elongation, it was reasonable to hypothesize that Has/aPKC_ϵ regulates the subcellular distribution of Had/Na⁺,K⁺ ATPase by directly phosphorylating this residue. In an in vitro assay, we could not detect direct phosphorylation of Had/Na⁺,K⁺ ATPase, which does not rule out the possibility that Has/aPKC_ϵ needs cofactors that were missing in our assay system. Furthermore, studies on whether or not Has/aPKC_ϵ phosphorylates the C-terminal domains of Had/Na⁺,K⁺ ATPase and whether or not there is an indirect effect of Has/aPKC_ϵ on the phosphorylation state of Had/Na⁺,K⁺ ATPase will provide additional insights into the mechanistic relationship of Has/aPKC_ϵ and Had/Na⁺,K⁺ ATPase during early heart morphogenesis.

The phenotypic similarities of *had* and *nok* mutants in heart morphogenesis and the more severe defects observed in *had;nok* double-deficient embryos suggest a common defect underlying the loss of myocardial morphogenetic potential. Our data indicate that weakening of tight junctions and ionic imbalances

in myocardial cells contribute to the severe heart elongation phenotype observed in embryos deficient in *had*, *nok*, and both. It is possible that correct ionic gradients, modulated by $\text{Had}/\text{Na}^+, \text{K}^+$ ATPase, stabilize the integrity of the tight junction, and that weakening of the tight junction, the paracellular diffusion barrier, may then enhance ionic gradient imbalances. We have previously shown that the heart beat rate is reduced by 20% in *had*^{la1} mutants (Shu et al., 2003). A similarly reduced heart beat rate is noted in *nok*^{ms20} mutants (118.3 ± 16.9 beats per minute [$n = 46$] vs. 142.8 ± 11.5 beats per minute in wt siblings [$n = 32$]), indicating a defective ionic balance or reduced Na pump activity. Interestingly, a junctional defect was also noted in *D. melanogaster* Na^+, K^+ ATPase mutants, suggesting that the role of Na^+, K^+ ATPase in maintaining the integrity of cellular junction barriers is evolutionarily conserved from *D. melanogaster* to fish (Genova and Fehon, 2003; Paul et al., 2003). Further studies are required to address the possible link between tight junctions and ionic gradients in the control of epithelial morphogenesis.

Materials and methods

Fish maintenance, stocks, and ouabain treatment

Zebrafish were maintained at standard conditions (Westerfield, 1994). Embryos were staged at 28.5°C (Kimmel et al., 1995) and according to somite number. The following fish strains were used: wt AB, *had*, *Tg(cmlc2:GFP)* (Huang et al., 2003), *had*^{la1}, *nok*^{ms20}, and *has*^{ms67}. Embryos were treated with ouabain as previously described (Shu et al., 2003).

DNA constructs and site-directed mutagenesis

Both wt and mutant forms of *had/Na⁺,K⁺ ATPase a1B1* were produced by PCR amplification from a full-length cDNA template, introducing the XhoI and XbaI restriction sites 5' and 3', respectively. Site directed mutagenesis was performed using the Quick Change kit (Stratagene) and constructs were subsequently subcloned into the pCS2 + HisMyc expression vector (Rohr et al., 2006). Primer sequences are available upon request. The shorter wt and mutant forms (*myc::had*^{ms98} and *myc::had*^{3A98}) were produced by PCR amplification of only the first 294 bp of the respective template clones, introducing a 3' stop codon and XhoI and XbaI restriction sites 5' and 3', and were subsequently subcloned into pCS2 + HisMyc. For the generation of chimeric constructs between $\alpha 1B1$ and $\alpha 2$, the first 294 bp of both genes were PCR amplified and blunt-ended ligated into the reciprocal PCR fragments lacking the 5'-end sequences.

Injections of mRNAs and antisense oligonucleotide morpholinos

Constructs were transcribed using the SP6 mMessage mMachine kit (Ambion). *Tg(cmlc2:GFP)* and *nok*^{ms20}/*Tg(cmlc2:GFP)* embryos were injected with 3.8–5 ng and 2.5 ng of *had*MO (Shu et al., 2003). For rescue experiments, 100 pg of mRNAs were injected. For overexpression, 150 pg of *HisMyc::had*^{ms98} or *HisMyc::had*^{3A98} mRNA and 150 pg of *HisMyc::had*^{wt} or *HisMyc::had*^{3A} mRNA were used. The heart tube phenotype was evaluated at 24 hpf. Data presented are the means of at least three independent experiments. Statistical comparisons of rescue efficiencies of wt against different mutant forms of protein were made by *t* tests, and $P < 0.05$ was considered statistically significant.

Immunohistochemistry and in situ hybridization

Whole-mount antibody stainings were performed as previously described (Horne-Badovinac et al., 2001). Samples were embedded in SlowFade Gold antifade reagent (Invitrogen). Transverse sectioning was performed according to Trinh and Stainier (2004). Sections were embedded in 1.5% low melting Agarose. All images were obtained at RT. Confocal images were obtained with a confocal microscope (TCS SP2; Leica) using 40× objective and 4× zoom, or with a confocal microscope (LSM 510 Meta; Carl Zeiss Microimaging, Inc.; Figs. 2 and 4) using 63× objective and 2× zoom. TCS SP2 and LSM 510 software were used to capture the images. Images were processed using Photoshop (Adobe). The following antibodies were used: rabbit anti-aPKC ζ (1:100; Santa Cruz Biotechnology, Inc.),

mouse anti-ZO-1 (1:200; Zymed Laboratories), mouse anti-Myc (1:200; Invitrogen), goat anti-rabbit RRX (1:200), and anti-mouse Cy5 (1:200; Jackson ImmunoResearch Laboratories).

Immunohistochemical quantification was performed by measuring membrane and cytoplasmic intensity with ImageJ freeware (W.S. Rasband, National Institutes of Health, Bethesda, MD; <http://rsb.info.nih.gov/ij/>). Membrane area was defined using aPKC membrane staining as a marker. Relative membrane versus cytoplasmic distribution of wt or 3A mutant Had protein was calculated by comparing the intensity of membrane area with the corresponding sum of total cytoplasmic plus membrane areas for each individual myocardial cell.

Whole-mount in situ hybridization was performed as previously described (Chen and Fishman, 1996). The antisense RNA probe used in this study was *cmlc2* (a gift from D.Y.S. Stainier, University of California, San Francisco, San Francisco, CA). Embryos were embedded in glycerol. Images were obtained at RT with a SV11 stereomicroscope (Carl Zeiss Microimaging, Inc.) using the 1.6× objective and 6.6× zoom with the AxioCam camera and Axiovision software (Carl Zeiss Microimaging, Inc.). Photos were processed using Photoshop.

Protein fractionation and Western blot analysis

Fractionation of 24 hpf zebrafish embryos was done essentially as previously described (Anzenberger et al., 2006). Membranes were probed with mouse anti-Myc antibody (1:1,000; Invitrogen). For loading and fractionation control, membranes were stripped and tested for acetylated tubulin (mouse antiacetylated tubulin; 1:1,000; Sigma-Aldrich).

Western blot quantification was performed by measuring band intensity with ImageJ freeware. Relative membrane versus cytoplasmic distribution of wt or 3A mutant Had protein was calculated by comparing the intensity of membrane fractions with the corresponding sum of total cytoplasmic plus membrane fractions.

had^{la1} and *nok*^{ms20} genotyping

For genotyping of 16-somite stage *nok*^{ms20} embryos, we made use of a Sall restriction site that is deleted by the mutation and performed PCR on tail tissue, followed by the Sall digest. DNA primers used for genotyping are available upon request. We also used RFLP to genotype the rescued *had*^{la1} mutant embryos as previously described (Shu et al., 2003).

In vitro kinase assay

For in vitro kinase assays, embryos were injected with 150 pg *HisMyc::had*^{ms98} or *HisMyc::had*^{3A98} mRNA at the one-cell stage. Embryo (24 hpf) extracts were prepared in lysis buffer (20 mM Tris-HCl, pH 7.5, 150 mM NaCl, 5 mM β -mercaptoethanol, 20 mM imidazole, 1% C12E10, 0.2 mM PMSF, protease inhibitor cocktail [Roche]). HisMyc-tagged fragments were purified using Ni-NTA columns (QIAGEN). In vitro kinase assays were performed on the eluted HisMyc-tagged protein. Samples were incubated at room temperature for 30 min with 50 ng human recombinant aPKC ζ (Calbiochem) or Has/aPKC ι in kinase reaction buffer (20 mM Tris-HCl, pH 8.0, 5 mM MgCl₂, 100 mM imidazole, 15% glycerol, 30 mM NaH₂PO₄, pH 8.0, 0.05% Tween 20, 50 μ M ATP, 5 μ Ci γ [³²P]-labeled ATP). Kinase reaction was stopped by adding 4× SDS loading buffer and boiling at 95°C for 5 min. We used the commercially available peptide epsilon (25 ng loaded per lane) as positive control for the kinase assay (Calbiochem). Samples were split in two, for autoradiography and for Western-blot analysis, and resolved in 18% acrylamide/bisacrylamide (29:1) gels. For detection of ³²P incorporation, the gel was dried and visualized by autoradiography. For Western blot analysis, the following antibodies were used: mouse anti-Myc (1:1,000; Invitrogen), rabbit anti-aPKC ζ (1:1,000; Santa Cruz Biotechnology, Inc.), goat anti-rabbit HRP (1:5,000; Pierce Chemical Co.), and goat anti-mouse HRP (1:10,000; Jackson ImmunoResearch Laboratories).

Recombinant Has/aPKC ι was generated by injecting embryos with 300 pg of *HisMyc::apkc ι* mRNA. Embryo (24 hpf) extracts were prepared in lysis buffer. HisMyc-tagged Has/aPKC ι protein was purified using Ni-NTA columns, and eluted in kinase elution buffer (20 mM Tris-HCl, pH 8.0, 300 mM NaCl, 5 mM MgCl₂, 100 mM imidazole, 30 mM NaH₂PO₄, pH 8.0, 0.05% Tween 20, and 30% glycerol).

Online supplemental material

Fig. S1 shows that the establishment of ZO-1-positive tight junction belts is not affected in *nok*^{ms20} mutants, *had* morphants, and *nok*^{ms20}/*had* double mutant/morphants at the 16-somite stage. Fig. S2 shows that the N-terminal tail of $\text{Had}/\text{Na}^+, \text{K}^+$ ATPase is not directly phosphorylated in vitro by Has/aPKC ι . Fig. S3 shows that the ATPase catalysis mutant *Had*^{D379N} is stable and correctly associates with membranes.

We are indebted to J. Eichhorst, D.Y.S. Stainier, H.J. Tsai, E. Wanker, and B. Wiesner for sharing reagents and tools, and to R. Fechner for expert technical assistance with the fish facility. C. Eichhorn helped with the statistical analysis of data. We would like to thank T. Willnow, M. Bader, and U. Ziebold for comments on the manuscript.

This work was supported, in part, by a presidential grant from the Helmholtz Society.

Submitted: 21 June 2006

Accepted: 8 December 2006

References

- Anzenberger, U., N. Bit-Avragim, S. Rohr, F. Rudolph, B. Dehmel, P. Haas, D. Gilmour, T.E. Willnow, and S. Abdelilah-Seyfried. 2006. Elucidation of Megalin/LRP2-dependent endocytic transport processes in the larval zebrafish pronephros. *J. Cell Sci.* 119:2127–2137.
- Bertorello, A.M., A. Aperia, S.I. Walaas, A.C. Nairn, and P. Greengard. 1991. Phosphorylation of the catalytic subunit of Na⁺,K⁺ ATPase inhibits the activity of the enzyme. *Proc. Natl. Acad. Sci. USA.* 88:11359–11362.
- Blanco, G., and R.W. Mercer. 1998. Isozymes of the Na⁺,K⁺ ATPase: heterogeneity in structure, diversity in function. *Am. J. Physiol.* 275:F633–F650.
- Chen, J., and M. Fishman. 1996. Zebrafish tinman homolog demarcates the heart field and initiates myocardial differentiation. *Development.* 122:3809–3816.
- Chibalin, A.V., A.I. Katz, P.O. Berggren, and A.M. Bertorello. 1997. Receptor-mediated inhibition of renal Na⁺,K⁺ ATPase is associated with endocytosis of its alpha- and beta-subunits. *Am. J. Physiol.* 273:C1458–C1465.
- Chibalin, A.V., C.H. Pedemonte, A.I. Katz, E. Feraille, P.O. Berggren, and A.M. Bertorello. 1998. Phosphorylation of the catalytic alpha-subunit constitutes a triggering signal for Na⁺,K⁺ ATPase endocytosis. *J. Biol. Chem.* 273:8814–8819.
- Genova, J.L., and R.G. Fehon. 2003. Neuroglian, gliotactin, and the Na⁺,K⁺ ATPase are essential for septate junction function in *Drosophila*. *J. Cell Biol.* 161:979–989.
- Horne-Badovinac, S., D. Lin, S. Waldron, M. Schwarz, G. Mbamalu, T. Pawson, Y. Jan, D.Y. Stainier, and S. Abdelilah-Seyfried. 2001. Positional cloning of *heart and soul* reveals multiple roles for PKC lambda in zebrafish organogenesis. *Curr. Biol.* 11:1492–1502.
- Huang, C.J., C.T. Tu, C.D. Hsiao, F.J. Hsieh, and H.J. Tsai. 2003. Germ-line transmission of a myocardium-specific GFP transgene reveals critical regulatory elements in the *cardiac myosin light chain 2* promoter of zebrafish. *Dev. Dyn.* 228:30–40.
- Hug, H., and T.F. Sarre. 1993. Protein kinase C isoenzymes: divergence in signal transduction? *Biochem. J.* 291:329–343.
- Hurd, T.W., L. Gao, M.H. Roh, I.G. Macara, and B. Margolis. 2003. Direct interaction of two polarity complexes implicated in epithelial tight junction assembly. *Nat. Cell Biol.* 5:137–142.
- Kimmel, C.B., W.W. Ballard, S.R. Kimmel, B. Ullmann, and T.F. Schilling. 1995. Stages of embryonic development of the zebrafish. *Dev. Dyn.* 203:253–310.
- Lopina, O.D. 2000. Na⁺,K⁺ ATPase: structure, mechanism, and regulation. *Membr. Cell Biol.* 13:721–744.
- Lowery, L.A., and H. Sive. 2005. Initial formation of zebrafish brain ventricles occurs independently of circulation and requires the *nagie oko* and *snakeheadatp1a1a.1* gene products. *Development.* 132:2057–2067.
- Nam, S.C., and K.W. Choi. 2003. Interaction of Par-6 and Crumbs complexes is essential for photoreceptor morphogenesis in *Drosophila*. *Development.* 130:4363–4372.
- Ohtsubo, M., S. Noguchi, K. Takeda, M. Morohashi, and M. Kawamura. 1990. Site-directed mutagenesis of Asp-376, the catalytic phosphorylation site, and Lys-507, the putative ATP-binding site, of the alpha-subunit of *Torpedo californica* Na⁺/K⁺-ATPase. *Biochim. Biophys. Acta.* 1021:157–160.
- Paul, S.M., M. Ternet, P.M. Salvaterra, and G.J. Beitel. 2003. The Na⁺,K⁺ ATPase is required for septate junction function and epithelial tube-size control in the *Drosophila* tracheal system. *Development.* 130:4963–4974.
- Peterson, R.T., J.D. Mably, J.N. Chen, and M.C. Fishman. 2001. Convergence of distinct pathways to heart patterning revealed by the small molecule centramide and the mutation *heart-and-soul*. *Curr. Biol.* 11:1481–1491.
- Rajasekaran, A.K., M. Hojo, T. Huima, and E. Rodriguez-Boulan. 1996. Catenins and zonula occludens-1 form a complex during early stages in the assembly of tight junctions. *J. Cell Biol.* 132:451–463.
- Rajasekaran, S.A., L.G. Palmer, S.Y. Moon, S.A. Peralta, G.L. Apodaca, J.F. Harper, Y. Zheng, and A.K. Rajasekaran. 2001a. Na⁺,K⁺ ATPase activity is required for formation of tight junctions, desmosomes, and induction of polarity in epithelial cells. *Mol. Biol. Cell.* 12:3717–3732.
- Rajasekaran, S.A., L.G. Palmer, K. Quan, J.F. Harper, W.J. Jr, W.J. Ball, N.H. Bander, S.A. Peralta, and A.K. Rajasekaran. 2001b. Na⁺,K⁺ ATPase beta-subunit is required for epithelial polarization, suppression of invasion, and cell motility. *Mol. Biol. Cell.* 12:279–295.
- Rajasekaran, S.A., J. Hu, J. Gopal, R. Gallemore, S. Ryazantsev, D. Bok, and A.K. Rajasekaran. 2003. Na⁺,K⁺ ATPase inhibition alters tight junction structure and permeability in human retinal pigment epithelial cells. *Am. J. Physiol. Cell Physiol.* 284:C1497–C1507.
- Rohr, S., N. Bit-Avragim, and S. Abdelilah-Seyfried. 2006. Heart and soul/PRKCi and nagie oko/Mpp5 regulate myocardial coherence and remodeling during cardiac morphogenesis. *Development.* 133:107–115.
- Shu, X., K. Cheng, N. Patel, F. Chen, E. Joseph, H.J. Tsai, and J.N. Chen. 2003. Na⁺,K⁺ ATPase is essential for embryonic heart development in the zebrafish. *Development.* 130:6165–6173.
- Suzuki, A., and S. Ohno. 2006. The PAR-aPKC system: lessons in polarity. *J. Cell Sci.* 119:979–987.
- Suzuki, A., T. Yamanaka, T. Hirose, N. Manabe, K. Mizuno, M. Shimizu, K. Akimoto, Y. Izumi, T. Ohnishi, and S. Ohno. 2001. Atypical protein kinase C is involved in the evolutionarily conserved par protein complex and plays a critical role in establishing epithelia-specific junctional structures. *J. Cell Biol.* 152:1183–1196.
- Therien, A.G., and R. Blosein. 2000. Mechanisms of sodium pump regulation. *Am. J. Physiol. Cell Physiol.* 279:C541–C566.
- Trinh, L.A., and D.Y. Stainier. 2004. Fibronectin regulates epithelial organization during myocardial migration in zebrafish. *Dev. Cell.* 6:371–382.
- Vasilets, L.A., G. Schmalzing, K. Madefessel, W. Haase, and W. Schwarz. 1990. Activation of protein kinase C by phorbol ester induces downregulation of the Na⁺,K⁺ ATPase in oocytes of *Xenopus laevis*. *J. Membr. Biol.* 118:131–142.
- Vasilets, L.A., H. Fotis, and E.M. Gartner. 1997. Regulatory phosphorylation of the Na⁺,K⁺ ATPase from mammalian kidneys and *Xenopus* oocytes by protein kinases. Characterization of the phosphorylation site for PKC. *Ann. N. Y. Acad. Sci.* 834:585–587.
- Vasilets, L.A., R. Postina, and S.N. Kirichenko. 1999. Mutations of Ser-23 of the alpha subunit of the rat Na⁺,K⁺ ATPase to negatively charged amino acid residues mimic the functional effect of PKC-mediated phosphorylation. *FEBS Lett.* 455:8–12.
- Wang, Q., T.W. Hurd, and B. Margolis. 2004. Tight junction protein Par6 interacts with an evolutionarily conserved region in the amino terminus of PALS1/stardust. *J. Biol. Chem.* 279:30715–30721.
- Westerfield, M. 1994. *The Zebrafish Book*. University of Oregon Press, Eugene.
- Yelon, D., S.A. Horne, and D.Y. Stainier. 1999. Restricted expression of cardiac myosin genes reveals regulated aspects of heart tube assembly in zebrafish. *Dev. Biol.* 214:23–37.
- Yuan, S., and E.M. Joseph. 2004. The small heart mutation reveals novel roles of Na⁺,K⁺ ATPase in maintaining ventricular cardiomyocyte morphology and viability in zebrafish. *Circ. Res.* 95:595–603.